Angewandte International Edition Chemie

DOI: 10.1002/anie.201006746

Nanocomposites

Completely Miscible Nanocomposites**

*Steffen Fischer, Andrea Salcher, Andreas Kornowski, Horst Weller, and Stephan Förster**

Polymer nanocomposites have gathered substantial academic and industrial interest since the first reports in the early 1990s.[1–3] Observations of large property changes at very low volume fractions of added nanoparticles and the possibility to integrate nanoparticles with specific properties providing new functions have motivated an increasing number of investigations.[4–6] Further progress in all areas is crucially limited by the strong tendency of nanoparticles to aggregate in polymeric matrices.[7] To achieve highly dispersed states in nanocomposites, in situ polymerization[8] and kinetic entrapment[9] techniques have been exploited. However, only a full thermodynamic compatibilization, which provides miscibility of the nanoparticles with the polymer matrix, makes the production of nanocomposites independent of the preparation procedure and provides long-term thermodynamic stability. We discovered that coating nanoparticles with a brush-like polymer layer provides a general and versatile route to fully miscible nanocomposites that show no nanoparticle aggregation over the whole range of nanoparticle volume fractions.

To prepare nanoparticles that are miscible with the polymer matrix, the nanoparticle surface has to be covered with a layer of a matrix-miscible polymer. Generally, this coating is still insufficient to provide complete miscibility because of the loss of conformational entropy of the matrix polymers close to the nanoparticle surface.[10] Owing to the large surface area of nanoparticles, this purely entropic effect alone leads to immiscibility and aggregation, a phenomenon that in colloidal solutions is known as depletion flocculation. To provide sufficient conformational freedom for the matrix polymers close to the nanoparticle surface, the polymer layer covering the nanoparticles should have a low segment density at its periphery to provide sufficient conformational freedom for the matrix polymers. This type of layer structure is ideally realized in spherical polymer brushes[11] and is schematically shown in Figure 1a. It could therefore be imagined that nanoparticles coated with a spherical brush-like polymer layer are completely miscible with the matrix polymer. Support for this idea is derived from recent studies on polymer-brush-coated nanoparticles in dilute solution[12] and in polymer matrices,[13] which indicated that spherical polymer brushes could suppress aggregation if the grafting density was sufficiently high. Herein, we demonstrate that spherical polymer-brush layers can indeed provide complete miscibility, even at the highest volume fractions of added nanoparticles, where the nanoparticles begin to assemble into ordered superlattices.

In a spherical polymer brush, the polymer chains are attached with one end to the particle surface. The chain ends may be attached covalently, but we found that a more versatile and simpler approach was to attach the polymers by coordinative interactions. The nanoparticles had very low polydispersities to facilitate packing at high nanoparticle volume fractions. To demonstrate the generality of the approach, we investigated nanocomposites with metal, oxide, sulfide, and selenide nanoparticles having catalytic, magnetic, and semiconducting properties. As matrix and layer polymer we used polystyrene, which has mechanical properties reaching from glassy to fluid and is noncrystalline, thus excluding interfering effects of nucleation and crystallization on nanocomposite properties. Polystyrene can be prepared with a narrow molecular-weight distribution and can be functionalized with end groups that coordinatively bind to the nanoparticle surface. In the present study we used diamine and carboxylic acid groups, but other groups such as thiols and phosphonates can also be used. The polymer chains were attached to the nanoparticles through a recently developed ligand-exchange procedure, where the surface-bound low-molecular-weight ligands present after nanoparticle synthesis are replaced by the polymeric ligands (see the Supporting Information).[14]

To confirm the stable attachment of the polymer chains and the brush-like layer structure, we dissolved the polystyrene-coated nanoparticles in toluene, which is a good solvent for polystyrene. Dynamic light scattering experiments (DLS) showed that the hydrodynamic diameter systematically increases with increasing molecular weight of the polystyrene ligands (Figure 1b), a typical feature of a spherical polymer-brush layer. With DLS, no free polystyrene chains could be detected. Figure 1b shows data for CdSe nanoparticles; further examples for other nanoparticles are given in the Supporting Information. Using small-angle X-ray scattering (SAXS), the thickness and density of the polymer layers in solution could be determined (see the Supporting Information).

We find that the attached polymer layer is also stable in the bulk state and effectively prevents nanoparticle aggregation. Figure 1c,d shows TEM images of F_3O_4 nanoparticles covered with oleic acid after synthesis and covered with a layer of polystyrene after ligand exchange. The attachment of

---

[*] Dr. S. Fischer, A. Kornowski, Prof. Dr. H. Weller
Institut für Physikalische Chemie, Universität Hamburg (Germany)
Prof. Dr. S. Förster
Physikalische Chemie I, Universität Bayreuth
Universitätsstrasse 30, 95447 Bayreuth (Germany)
E-mail: stephan.foerster@uni-bayreuth.de
Dr. A. Salcher
Centrum für Angewandte Nanotechnologie, Hamburg (Germany)

[**] We thank Hauke Heller and Marie Pelletier for providing the FePt and PbS nanoparticles and Ullrich Tromsdorf and Elmar Pöselt for helpful support for the nanoparticle synthesis.

Supporting information for this article is available on the WWW under http://dx.doi.org/10.1002/anie.201006746.

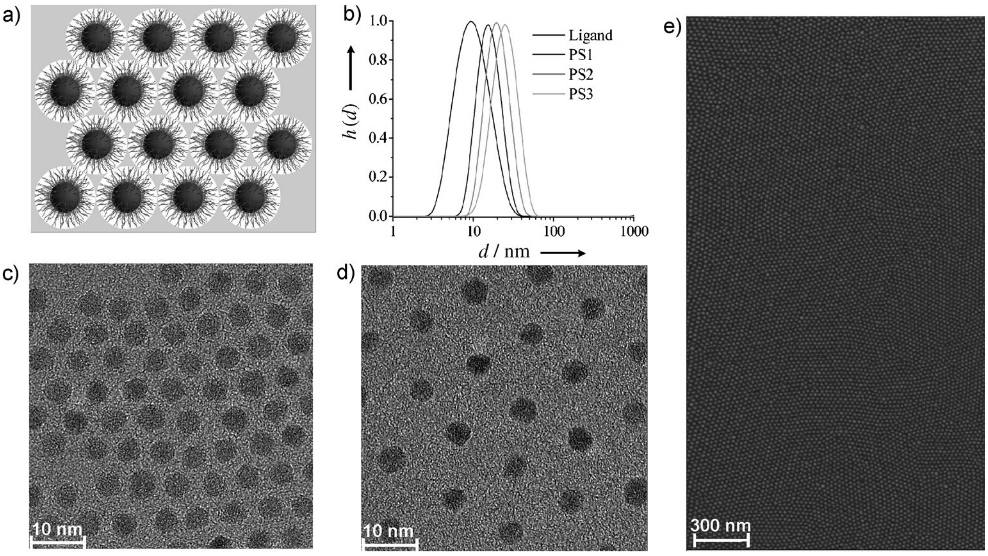

Figure 1. a) Schematic diagram of a nanocomposite consisting of nanoparticles coated with brush-like layers. b) Hydrodynamic diameters of CdSe nanoparticles coated with polystyrene of different molecular weights. PS1 3200 g mol^{-1}, PS2 7600 g mol^{-1}, PS3 15600 g mol^{-1}. c, d) TEM images of Fe_3O_4 nanoparticles covered with a layer of oleic acid directly after synthesis (c) and coated with a layer of polystyrene (PS2 7600 g mol^{-1}) after ligand exchange (d). The increased distance between the nanoparticles can be clearly observed. e) SEM image of a large sample area showing the stability of the nanoparticles against aggregation at high nanoparticle volume fractions.

the polymer chains leads to a considerable increase of the interparticle distance. The SEM image in Figure 1 e shows that there are no signs of aggregation at high nanoparticle volume fractions.

These fully compatibilized nanocomposites allowed for the first time a systematic investigation of the dynamic mechanical properties of a nanocomposite as a function of the volume fraction of added nanoparticles. For this study, we used polystyrene-coated Fe_3O_4 nanoparticles with radii of 2.7 nm, which were synthesized with low polydispersity on a multigram scale[15] sufficient to prepare nanocomposites for bulk rheological measurements. The polystyrenes used for the nanoparticle coating and the matrix polymer were from the same batch synthesized by anionic polymerization and had the same molecular weight with narrow molecular-weight distribution. Measurements were performed from 70–250 °C to cover the range from the glassy to the melt state. To verify that the nanoparticles were singly dispersed within the nanocomposite during the course of the measurements, we performed SAXS measurements before and after the investigations (see the Supporting Information). We investigated nanocomposites covering the complete range from pure homopolymer to pure polymer-coated nanoparticles, corresponding to a range of nanoparticle volume fractions of $0 \leq \phi \leq 0.089$. Higher volume fractions up to $\phi = 0.3$ can be realized with shorter polymer chains (see also Figure 3 b), with an upper limit of $\phi = 0.63$ for the nanoparticles coated with low-molecular-weight ligand.

Figure 2 a shows the measured values of storage modulus G' at a temperature of 100 °C, which is the glass-transition temperature of the matrix polymer. At high frequencies, where the matrix is in the glassy state, there is no effect of added nanoparticles on the measured storage modulus, even for the highest nanoparticle volume fractions (see arrow). The situation is different at lower frequencies, where the matrix responds viscoelastically. This effect becomes even more pronounced at higher temperatures. A measurement at 120 °C (Figure 2 b) shows that even at the lowest volume fractions there is a considerable increase of the measured storage modulus. We observe that at a volume fraction of polymer-coated nanoparticles of only 5 %, which corresponds to a volume fraction of bare nanoparticles of 0.5 %, the storage modulus is increased by 300 %. At higher volume fractions the storage modulus increases by four orders of magnitude (see arrow in Figure 2 b). These measurements reveal that the large increase of the storage modulus with increasing nanoparticle volume fraction is related to a reduced mobility of the polymer chains caused by the nanoparticles. At volume fractions above $\phi = 0.02$ the nanoparticles begin to interact, leading to localization of the nanoparticles and solidification of the nanocomposite. Nanoparticle localization can be observed from the development of Bragg peaks with increasing volume fractions, as shown in Figure 3 a. The interactions

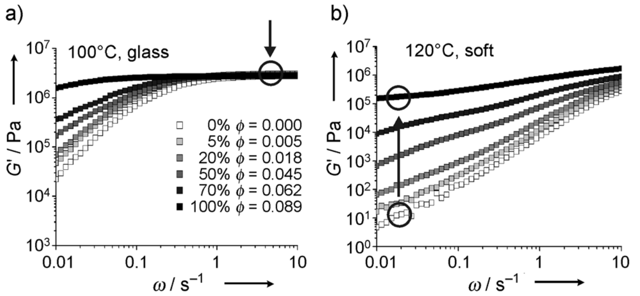

Figure 2. a) Storage modulus $G'(\omega)$ for the Fe_3O_4–polystyrene nanocomposites measured over a range of nanoparticle volume fractions ϕ from the pure homopolymer ($\phi = 0.000$) to the pure polymer-coated nanoparticles ($\phi = 0.089$; PS9 MW = 8600 g mol^{-1}). At 100 °C and high frequencies, where the polystyrene matrix is in its glassy state, added nanoparticles have no effect on the storage modulus G' (see arrow). b) At 120 °C, where the polystyrene matrix becomes soft, an increase of the storage modulus over four orders of magnitude can be observed with increasing volume fraction of the nanoparticles (see arrow). The same color code is used in (a) and (b).

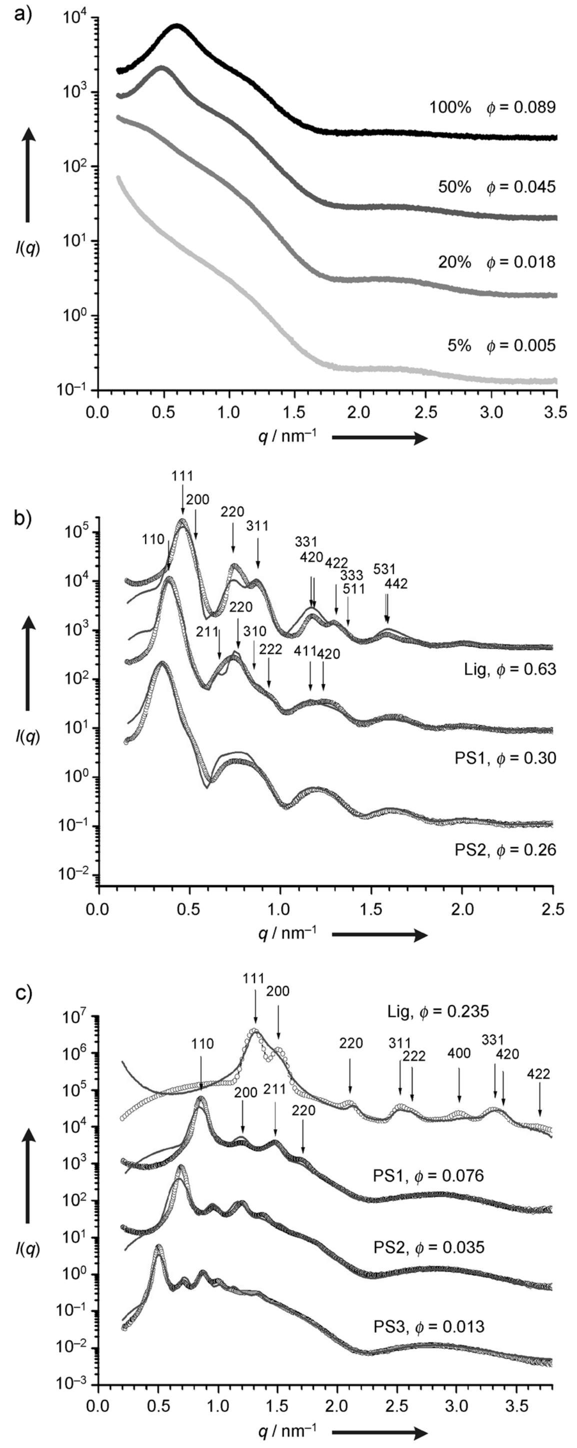

Figure 3. a) Small-angle X-ray scattering (SAXS) curves showing the development of a Bragg peak with increasing nanoparticle volume fraction ϕ owing to localization of the nanoparticles. (Same samples and color code as in Figure 2 are used.) b, c) SAXS curves measured for Fe_3O_4 (b) and CdSe nanocomposites (c) in the ordered state. The positions of the reflections indicate face-centered cubic (fcc) packing for the low-molecular-weight ligands and body-centered cubic (bcc) packing for the polymeric ligands. The oscillations arising from the nanoparticle form factor are well-resolved, showing that aggregation is absent. The nanocomposites in (b) and (c) are made from pure polymer-coated nanoparticles, where the volume fraction and the interparticle distance can be directly controlled by the length of the attached polymer ligands over a range of $\phi = 0.01$–0.30 corresponding to interparticle distances of 5–20 nm. Lig = low-molecular-weight ligand. PS1 3200 g mol^{-1}, PS2 7600 g mol^{-1}, PS3 15600 g mol^{-1}.

are mediated by the attached polymer layer and thus occur even at very low volume fractions of added nanoparticles.

Solidification is accompanied by ordering of the nanoparticles within the polymer matrix, as shown by the measured SAXS curves in Figure 3b,c. For these nanocomposites, which consist of the pure polymer-coated nanoparticles without added homopolymer, the variation of the nanoparticle volume fraction can be directly controlled by the molecular weight of the attached polymer chains in a range of $\phi = 0.013$–0.3, corresponding to a variation of the interparticle distance between 5 and 20 nm. Examples are shown for polystyrene-coated Fe_3O_4 (Figure 3b) and CdSe nanoparticles (Figure 3c). Further examples for PbS and FePt nanoparticles are given in the Supporting Information. These studies show that ordering can occur at extremely small volume fractions of $\phi \approx 0.01$ for high-molecular-weight polymers. The peak positions and the fits to the scattering curves (solid lines)[16,17] show the formation of highly ordered fcc lattices for the nanoparticles coated with low-molecular-weight ligand and bcc lattices for the polymer-coated nanoparticles. Bcc lattices are typical for systems interacting through soft potentials, which reflects the low segment density at the periphery of the polymer layer. Particles with hard-sphere interactions form fcc lattices.[18] The degree of order is remarkable, and it is better than the order achieved recently with gold–DNA nanocomposites.[19,20] The possibility to control the interparticle distance in the range of 5–20 nm is of great relevance for nanocomposites in magnetic storage and photovoltaic devices, where this is the critical length scale for dipolar magnetic interactions and exciton diffusion.

In summary, we describe for the first time a route to fully compatibilized nanocomposites showing no aggregation even at the highest volume fractions. Dynamic mechanical experiments reveal that the addition of nanoparticles retards the polymer chain dynamics of the nanocomposite, thus leading to solidification and ordering at very low volume fractions. The studies represent a breakthrough for the preparation of compatible nanocomposites and provide a key step for interparticle separation control of nanoparticles in nanocomposites in a size range relevant for applications in magnetic storage and photovoltaic devices.

Received: October 27, 2010
Revised: February 9, 2011

Keywords: nanocomposites · nanoparticles · polymers · rheology

[1] A. Usuki, Y. Kojima, M. Kawasumi, A. Okada, Y. Fukushima, T. Karauchi, O. Kamigaito, *J. Mater. Res.* **1993**, *8*, 1179.

[2] R. A. Vaia, H. Ishii, R. A. Giannelis, *Chem. Mater.* **1993**, *5*, 1694.

[3] T. P. Lan, T. J. Pinnavaia, *Chem. Mater.* **1994**, *6*, 2216.

[4] A. C. Balazs, T. Emrick, T. P. Russell, *Science* **2006**, *314*, 1107–1110.

[5] D. R. Paul, L. M. Robeson, *Polymer* **2008**, *49*, 3187–3204.

[6] K. I. Winey, R. A. Vaia, *MRS Bull.* **2007**, *32*, 314.

[7] R. A. Vaia, H. D. Wagner, *Mater. Today* **2004**, *7*, 32–37.

[8] Y. Lu, Y. Yang, A. Sellinger, M. Lu, J. Huang, H. Fan, R. Haddad, G. Lopez, A. R. Burns, D. Y. Sasaki, J. Shelnutt, C. J. Brinker, *Nature* **2001**, *410*, 913–917.

[9] S. M. Liff, N. Kumar, G. H. McKinley, *Nat. Mater.* **2007**, *6*, 76–83.

[10] P. G. deGennes, *Scaling Concepts in Polymer Physics*, Cornell University Press, **1979**.

[11] S. T. Milner, *Science* **1991**, *251*, 905.

[12] M. S. Nikolic, A. Kornowski, A. Rank, R. Schubert, A. Frömsdorf, H. Weller, S. Förster, *Angew. Chem.* **2009**, *121*, 2790; *Angew. Chem. Int. Ed.* **2009**, *48*, 2752.

[13] P. Akcora, H. Liu, S. K. Kumar, J. Moll, Y. Li, B. C. Benicewicz, L. S. Schadler, D. Acehan, A. Z. Panagiotopoulos, V. Pryamitsyn, V. Ganesan, J. Ilavsky, P. Thiyagarajan, R. H. Colby, J. F. Douglas, *Nat. Mater.* **2009**, 8, 354.

[14] M. A. Nikolic, V. Alexandrovic, M. Krack, A. Kornowski, S. Förster, H. Weller, *Angew. Chem.* **2006**, *118*, 6727; *Angew. Chem. Int. Ed.* **2006**, *45*, 6577.

[15] J. Park, K. An, Y. Hwang, J.-G. Park, H.-J. Noh, J.-Y. Kim, J.-H. Park, N.-M. Hwang, T. Hyeon, *Nat. Mater.* **2004**, *3*, 891–895.

[16] S. Förster, A. Timmann, M. Konrad, C. Schellbach, A. Meyer, S. S. Funari, P. Mulvaney, R. Knott, *J. Phys. Chem. B* **2005**, *109*, 1347.

[17] S. Förster, L. Apostol, W. Bras, *J. Appl. Crystallogr.* **2010**, *43*, 639.

[18] G. A. McConnell, A. P. Gast, J. S. Huang, S. D. Smith, *Phys. Rev. Lett.* **1993**, *71*, 2102–2105.

[19] W. Cheng, M. J. Campolongo, J. J. Cha, S. J. Tan, C. C. Umbach, D. A. Muller, D. Luo, *Nat. Mater.* **2009**, *8*, 519–525.

[20] W. Cheng, M. R. Hartman, D.-M. Smilgies, R. Long, M. J. Campolongo, R. Li, K. Sekar, C.-Y. Hui, D. Luo, *Angew. Chem.* **2010**, *122*, 390–394; *Angew. Chem. Int. Ed.* **2010**, *49*, 380–384.